Updated atmospheric speciated mercury emissions from iron and steel production in China during 2000-2015

Qingru Wu[1,2], Wei Gao[1,2], Shuxiao Wang[1,2*], Jiming Hao[1,2]

[1]School of Environment, and State Key Joint Laboratory of Environment Simulation and Pollution Control, Tsinghua University, Beijing 100084, China

[2]State Environmental Protection Key Laboratory of Sources and Control of Air Pollution Complex, Beijing 100084, China

Correspondence to: S. X. Wang (shxwang@tsinghua.edu.cn)

9   **Abstract**

10   Iron and steel production (ISP) is one of the significant atmospheric Hg emission sources

11   in China. Atmospheric mercury (Hg) emissions from ISP during 2000-2015 were estimated by

12   using a technology-based emission factor method. To support the application of this method,

13   databases of Hg concentrations in raw materials, technology development trends, and Hg

14   removal efficiencies of air pollution control devices (APCDs) were constructed through

15   national sampling and literature review. Hg input to ISP increased from 21.6 t in 2000 to 94.5

16   t in 2015. In the various types of raw materials, coking coal and iron concentrates contributed

17   35%-46% and 25%-32% of the total Hg input. Atmospheric Hg emissions from ISP increased

18   from 11.5 t in 2000 to 32.7 t in 2015 with the peak of 35.6 t in 2013. Pollution control

19   promoted the increase of average Hg removal efficiency, from 47% in 2000 to 65% in 2015.

20   During the study period, sinter/pellet plant and blast furnace were the largest two emission

21   processes. However, emissions from roasting plant and coke oven cannot be ignored, which

22   accounted for 22%-34% of ISP's emissions. Overall Hg speciation shifted from 50/44/6

23   (gaseous elemental Hg (Hg^0) / gaseous oxidized Hg (Hg^{II}) / particulate-bound Hg (Hg_p)) in

24   2000 to 40/59/1 in 2015, which indicated higher proportion of Hg deposition around the

25   emission points. Future emissions of ISP were expected to decrease based on the

26   comprehensive consideration crude steel production, steel scrap utilization, energy saving,

27   and pollution control measures.

1 Introduction

China is the largest iron and steel production (ISP) country in the world. Crude steel production has increased from 127 Mt in 2000 to 804 Mt in 2015 (CISIA, 2001-2016). Rapid economic development has led to large emissions of air pollutants including mercury (Hg) emissions of ISP (Liu et al., 2016; Wang K. et al., 2016; Wang et al., 2014). To reduce Hg pollution, it is important to quantify atmospheric Hg emissions from ISP.

According to existing national inventories, atmospheric Hg emissions from ISP increased from 4.9 t in 1999 to 25.5 t in 2010 (AMAP/UNEP, 2008; Streets et al., 2005; Wu et al., 2006; Zhang et al., 2015a). In these studies, Hg emissions were determined as the product of crude steel production and unique emission factor of 0.04 g/t steel produced which did not consider the emissions from roasting plant and coke oven (two processes of ISP). However, field experiments in China's ISP indicated that these two processes are significant for Hg emissions. Emissions from coke oven accounted for 17%-49% of the total Hg emissions of ISP (Wang F. Y. et al., 2016). Thus, these two processes are potentially important in shaping the trends of ISP Hg emissions. Later long-term emission inventories revised the unique emission factor with dynamic factors by adopting transformed normal distribution function (Tian et al., 2015; Wang K. et al., 2016; Wu et al., 2016). Such method was based on the assumption that the emission factor was gradually improved according to the simulation curve and attempted to simulate the impact of technology improvement and pollution control on emission factor variation. However, the emission factors actually did not link with technology and APCDs directly. Thus, the simulated emission factors may be quite different from actual situation during a certain period (e.g. ten years) when technology and APCDs experienced dramatic change (Wu et al., 2016), especially under the background of tightening requirement of environmental protection in China in the past decades (MEP, 2011; NEA, 2014; SC, 2013). Recent global Hg assessment report applied a technology-based emission factor method to estimate the emissions of global ISP including China's (AMAP/UNEP, 2013). However, most of the parameters were from developed countries, which may impact the accuracy of emissions from developing countries such as China. In addition, emissions from roasting plants and arc steel making process (using scrap to produce steel) were not calculated in the

58   report.

59   The dominant parameters of a technology-based emission factor included Hg removal

60   efficiencies of APCDs and Hg concentrations in raw materials (Wu et al., 2016; Wu et al.,

61   2012; Zhang et al., 2015a). As to Hg removal efficiencies of APCDs, we hypothesized that the

62   use of data from recent field experiments on atmospheric Hg emission characteristics in

63   China's ISP will provide a foundation for the technology-based emission factor model (Wu et

64   al., 2016; Wu et al., 2012; Zhang et al., 2015a). However, current studies cannot support the

65   construction of Hg concentration databases for raw materials. Various raw materials were

66   used in ISP, covering iron concentrates, iron block, alloy materials, steel scrap, coal, and

67   additives (mainly limestone and dolomite). Field experiments in three China's steel smelters

68   indicated that the concentrations of iron concentrates were in the range of 23-66 ng/g (Wang

69   F.Y. et al., 2016; Zhang et al., 2015b). However, the Hg concentration data from limited

70   samples may lead to large uncertainty of the national inventory. Many studies have reported

71   Hg concentrations in coal (Swaine, 1992; Tian et al., 2010; USGS, 2004; Zhang et al., 2012).

72   But the specific requirement of low-sulfide coal (less than 1.2%) in ISP may lead to different

73   Hg concentrations in the consumed coal (Tao and Wang, 1994), since low-sulfide coal was

74   generally companied by low-Hg (Zhang, 2012). Rare studies have reported Hg concentrations

75   in steel scrap and dolomite. Therefore, constructing Hg concentration databases of raw

76   materials was the base to apply a technology-based emission factor model for China's ISP.

77   In this study, a technology-based emission factor model was constructed to estimate

78   atmospheric Hg emissions from China's ISP. To fulfill this aim, raw materials consumed in

79   steel smelters have been sampled and Hg concentrations have been analyzed to construct the

80   Hg concentration databases. Up-to-date Hg removal efficiencies from field experiments and

81   the development trends of production technology and APCDs have been summarized to

82   support the application of emission factor model.

83   **2   Methodology**

84   **2.1 Technology-based emission factor model for ISP**

85   Generally speaking, ISP method included long process steel making method and short

86 process steel making method. The long process steel making method included roasting plant,

87 coke oven, sinter/pellet plant, blast furnace, and oxygen steel making (**Fig. 1**). The short

88 process steel making method produced crude steel mainly from steel scrap in arc steel making

89 process directly.

90   Thus, atmospheric Hg emissions from ISP by province can be calculated as follows.

$$
\begin{aligned}
E_i(t) &= E_{i,l}(t) + E_{i,s}(t) \\
&= E_{i,l,r}(t) + E_{i,l,c}(t) + E_{i,l,p}(t) + E_{i,l,b}(t) + E_{i,l,o}(t) \\
&\quad + E_{i,s,a}(t)
\end{aligned}
\tag{E1}
$$

91   where, E was atmospheric Hg emissions from ISP, t; i was province; t referred to studied

92 year; l and s referred to long and short process steel making method; r, c, p, b, o, a referred to

93 roasting plant, coke oven, sinter/pellet plant, blast furnace, oxygen steel making, and arc steel

94 making.

95   For each process x, the technology-based emission factor and speciated Hg emissions

96 can be calculated as follows.

$$
EF_{i,x,k}(t) = \sum_j C_{i,x,j} \times M_{i,x,j}(t) \times S_i(t)^{-1} \times \gamma_x \times \sum_m \theta_m(t) \times \delta_{k.m} \times (1 - \eta_m) \times 1000^{-1}
\tag{E2}
$$

$$
E_{i,x,k}(t) = EF_{i,x,k}(t) \times S_i(t)
\tag{E3}
$$

97   where, EF was emission factor, g/t; x was studied process; k was speciated Hg; j was the

98 type of consumed raw material; C was Hg concentration in the consumed raw material, ng/g

99 (see section 2.2.1); M was the consumption of raw material, Mt (see section 2.2.2); S was the

100 production of crude steel, Mt (see section 2.2.2). γ was Hg release rate, which meant the

101 percentage of Hg released to flue gas from raw material, %. Hg release rate were collected

102 from field experiment studies (**Table S1**). That was 98% for roasting plant, 80% for coke

103 oven, 85% for sinter/pellet plant, 98% for blast furnace, 80% for oxygen steel making furnace,

104 and 95% for arc steel making furnace. m referred to the type of APCD combination (see

105 section 2.2.3); δ was the proportion of different Hg speciation (see section 2.2.3), %; θ was

106 the application rate of different APCD combinations (see section 2.2.3), %; η was Hg removal

107 efficiency (see section 2.2.3), %.

108 **2.2 Parameters for model**

109 2.2.1 Hg concentrations in raw materials

110   For the long process steel making method, the dominant raw materials included iron

111 concentrates, iron block, coal, limestone, dolomite, alloy, and steel scrap (**Fig. 1**). In the

112 roasting plant, limestone and dolomite were roasted together or separately to make quick lime

113 and caustic dolomite. In the coke oven, washed coal was used to produce coke. In the

114 sinter/pellet plant, iron-containing materials (mainly iron concentrates), quick lime, caustic

115 dolomite, and produced coke (mainly coke breeze) were mixed to produce sintered/pellet

116 block, which were used as raw materials with coal and produced coke in the blast furnace.

117 The produced pig iron from blast furnace and additional scraps were used to produce steel in

118 the oxygen steel making processes. For the short process steel making method, arc steel

119 making process was applied to produce steel by mainly using scraps as raw materials. In each

120 process, Hg input due to the use of intermediated products (e.g., quick lime, caustic dolomite,

121 and coke) was calculated by using mass balance method (Wu et al., 2012).

122   National sampling and Hg concentration analysis were conducted to construct the Hg

123 concentration databases for the consumed raw materials. The sampling, preparation and

124 analysis methods were described in detail in our previous studies (Wu et al., 2012; Zhang et

125 al., 2012). Lumex 915M + pyro attachment (with a detection limit of 0.5 ng/g) was applied to

126 analyze Hg concentration by using U.S. EPA Method 7473 (US EPA, 1998). Number of

127 samples and Hg concentrations in dominant raw materials by province were shown in **Table 1**.

128 National Hg concentrations (median value) in the consumed iron ores were 20 (0.6-387) ng/g,

129 which were lower than the median value of 30 (0.6-600) ng/g used in the global assessment

130 report (AMAP/UNEP, 2013). Overall Hg concentrations in the consumed coking coal (82

131 ng/g) and pulverized coal injection (PCI) coal (73 ng/g) were lower than the 170 (8-2248)

132 ng/g (Zhang, 2012) used in China's coal combustion sectors but higher than the 55 (50-60)

133 ng/g of global assessment report. Hg concentrations in the limestone were 18 (0.9-2753) ng/g.

134 Although the median value was lower than value of 30 (20-50) ng/g applied in the global

135 assessment report, the variation range was much wider according to our analysis. Hg

136 concentrations (median value) in the dolomite and iron block were 9 ng/g and 19 ng/g. In

137 oxygen and arc steel making processes, the main iron-containing materials were steel scrap,

138 alloy scrap, and pig iron. Hg concentrations (median value) in steel scrap and alloy scrap were

139 48 and 2 ng/g while the concentrations in pig iron were less than detection limit. For province

140 with samples no less than 15, the distribution characteristics of Hg concentrations of the

141 samples were generated by using the batch fit function of Crystalball software. Otherwise, Hg

142 concentrations were assumed to fit normal distribution.

143 2.2.2 Provincial consumptions of raw materials

144 Provincial consumptions of raw materials in 2015 were shown in **Table S2**. National

145 limestone consumptions were converted from quick lime consumptions (Ma, 2011) by using

146 the factor of 1.95 t limestone to produce 1 t quick lime (CISIA, 2001-2016) (**Table S3**).

147 National dolomite consumptions were derived from China steel statistics report (Ma, 1995)

148 according to the production trends of crude steel. The limestone and dolomite can be

149 consumed in the roasting and sinter/pellet plant. In the sinter/pellet plants, additives

150 (including limestone and dolomite) consumptions were approximately 153.9 kg/t sinter

151 produced or 10.5 kg/t pellet produced (CISIA, 2001-2016). We assumed that 88% of the

152 additives were limestone and 12% were dolomite according to field experiments (Wang F. Y.

153 et al., 2016). The rest of limestone and dolomite were consumed in the roasting plants.

154 Provincial consumptions of limestone and dolomite were distributed according to the

155 proportions of provincial pig iron productions in national production (Table S2). Provincial

156 pig iron productions were collected directly from yearbooks (CISIA, 2001-2016).

157 Provincial coking coal consumptions were converted from provincial coke consumptions

158 (CISIA, 2001-2016). Generally, there were two main types of coke production methods,

159 including machining coke production method and indigenous coke production method. Coal

160 consumptions were 1.35 t to produce 1 t of machining coke or 1.65 t to produce 1 t of

161 indigenous coke (UNEP, 2013; Wang, 1991). The produced cokes were used as raw materials

162 in both sinter/pellet plant and blast furnace. Provincial coke consumptions in blast furnace

163 were converted according coke ratio of 363-388 kg coke per t pig iron produced (CISIA,

164 2001-2016). The rest of cokes were assumed to be consumed in sinter/pellet plant.

165 National iron concentrate consumptions were converted from sinter/pellet productions.

166   Approximately 0.91-0.92 t and 0.96-0.97 t of iron concentrates were needed to produce 1 t

167   sinter and 1 t pellet, respectively (CISIA, 2001-2016). National sinter and pellet productions

168   were obtained directly from yearbooks (CISIA, 2001-2016) and provincial data were

169   converted according to provincial pig iron productions.

170   National PCI coal consumptions in blast furnace were collected from national energy

171   statistical yearbook (NESA, 2001-2016) and the provincial data were converted according to

172   provincial pig iron productions. The iron block consumption in blast furnace were converted

173   from pig iron production by using the factor of 156 kg iron block per t pig iron produced

174   (CISIA, 2001-2016).

175   The steel scrap was consumed in both oxygen and arc steel making process.

176   Consumptions of steel scrap in oxygen and arc steel making process were approximately 59.4

177   and 361.9 kg/t crude steel produced. Alloy consumptions to produce per t crude steel were

178   16-17 kg in oxygen steel making process and 140-156 kg in arc oxygen making process.

179   Oxygen and arc steel productions were collected directly from yearbooks (CISIA, 2001-2016).

180   Based on these ratios, provincial steel scrap and alloy consumptions were converted from

181   provincial crude steel productions.

182   2.2.3 Application rate, Hg removal efficiency, and Hg speciation

183   In the roasting plant, blast furnace, and steel making process, dust collectors such as

184   venturi, cyclone (CYC), wet scrubber (WS), electrostatic precipitator (ESP), and fabric filter

185   (FF) were used for flue gas dedusting. In coke oven process, washed coal were consumed and

186   the flue gas was cleaned with dust collectors or with additional washing scrubbers. For flue

187   gas from sinter/pellet plant, they were generally cleaned with dust collectors. Additional flue

188   gas desulfurization towers (FGD) were gradually applied after 2010. It should be noted that

189   the flue gas after dust collectors were generally collected as coal gas in gasometer. However,

190   rare APCDs were applied during the coal gas usage process. Thus, we assumed that all Hg in

191   the coal gas was emitted to air. The application rates of different APCD combinations by

192   process during 2005-2010 were collected from previous studies (Wang et al., 2014; Zhao et

193   al., 2013). The data of 2000-2004 and 2011-2015 were mainly derived from yearbooks

194   (CISIA, 2001-2016; NBS, 2001-2016) (Table S4). Hg removal efficiencies and speciation

195 profiles of APCDs (**Table S4**) were collected from field experiments and literature on

196 emission studies (Gao, 2016; Wang F. Y. et al., 2016; Zhang et al., 2015b). The distribution

197 characteristics of Hg removal efficiencies were assumed to fit normal distribution

198 characteristics.

199 **2.3 Uncertainty analysis**

200   Monte Carlo simulation was introduced to estimate the uncertainty of emissions.

201 Detailed description of the simulation processes has been reported in our previous studies

202 (Hui et al., 2016; Wu et al., 2016; Zhang et al., 2015a). In this study, the (P50-P10)/P50 and

203 (P90-P50)/P50 values were still regarded as lower and upper limits of uncertainties with 80%

204 confidence degree, where P10, P50, and P90 meant that the probabilities of actual results

205 lower than corresponding values were 10%, 50%, and 90%, respectively.

206 **3 Results and Discussion**

207 **3.1 Hg input trends**

208   Hg input to ISP increased from 21.6 t in 2000 to 94.5 t in 2015 (**Fig. 2**). The peak of Hg

209 input was in 2014 when the crude steel production reached the highest value (**Table S3**).

210 During 2000-2014, the average annual growth rate (AAGR) of Hg input was 11% while Hg

211 input reduced by 3% from 2014 to 2015. In the various types of raw materials, coking coal

212 and iron concentrates contributed the largest amount of Hg input, accounting for 35%-46%

213 and 25%-32% of the total, respectively. Hg input due to the use of coking coal increased from

214 9.9 t in 2000 to 33.5 t in 2015. Hg input with iron concentrates increased at AAGR of 12%

215 from 2000 and reached 29.2 t in 2015. The PCI coal brought approximately 6%-9% of Hg to

216 ISP. Hg in the additives (including limestone and dolomite) contributed 12%-18% of total Hg

217 input. Hg in the iron block was in the range of 0.6-3.6 t. Hg input due to the use of steel scrap

218 and alloy was 4.1 t in 2015, accounting for 4% of national total. However, steel scrap and

219 alloy contributed 7% of total crude steel production in 2015 (CISIA, 2016).

3.2 Hg emission trends

3.2.1 Hg emission trends by process

Atmospheric Hg emissions from ISP increased from 11.5 t in 2000 to 32.7 t in 2015 (**Fig. 3**). The peak of emissions was in 2013 when the emissions reached 35.6 t. In 2015, emissions from long process steel making method and short process steel making were 32.2 t and 0.5 t, accounting for 98.3% and 1.7% of national total, respectively. Thus, emissions from long process steel making were still the dominant emission process of China's ISP. Among the processes, emissions from sinter/pellet plant accounted for 42%-49% of annual total. Its emissions increased from 4.8 t in 2000 at the AAGR of 10.1% and reached 15.9 t in 2015. Blast furnace was also significant Hg emission process. Its emissions increased from 1.9 t in 2000 to 7.9 t in 2015 at AAGR of 10.0%. AAGR for roasting plant and coke oven was 8.3% and 1.2%. In 2015, both emissions from roasting plant and coke oven were 3.5 t, respectively.

The slower AAGR of Hg emissions (7.2%) than that of crude steel production (13%) reflected the impact on Hg emission reduction due to energy saving and environmental protection in ISP. On one hand, Hg input to produce unitary crude steel decreased from 0.17 to 0.12 g/t, which mainly benefited from the improvement of coke production efficiency and energy utilization efficiency of sinter/pellet plant and blast furnace. Since 2004, indigenous coke production method with high coal consumption has been gradually replaced with machine coke production method. The coke ratio in sinter/pellet plant has been reduced from approximately 388 kg/t pig iron produced in 2000 to 363 kg/t in 2015 (CISIA, 2001-2016). On the other hand, the improvement of APCDs increased the overall Hg removal efficiency from 47% in 2000 to 65% in 2015 (**Fig. 3**). APCDs for coke oven have shown the largest Hg removal efficiencies (64%-87%) while pollution control in sinter/pellet plant contributed most to the rapid Hg reduction speed during 2000-2015. The replacement of CYC and WS with ESP and FF in sinter/pellet plant improved Hg removal efficiency from 21% in 2000 to 44% in 2010. The application of FGD in addition to dust collectors was the main driver of Hg reduction in sinter/pellet process during 2011-2015. Hg removal efficiency in sinter/pellet plant was 53% in 2015.

248   3.2.2 Hg emission trends by province

249   Provincial Hg emissions in 2000, 2005, 2010, and 2015 were shown in **Table 2**. In 2000,

250   Shanxi, Shanghai, Henan, Hebei, and Shandong were the top five largest emitters with

251   emissions larger than 1 t. Emissions from these five provinces contributed to 58% of national

252   Hg emissions. Following these five provinces were Liaoning, Beijing, Gansu, Jiangsu, and

253   Jiangxi. Summation of the emissions from all the above ten provinces were 9.0 t, accounting

254   for 78% of national emissions in 2000. At the provincial level, we noted significant

255   differences of Hg emission trends during the past 16 years. The AAGR of provincial Hg

256   emissions varied from -40% to 26%. Negative AAGR existed in Beijing and Shanghai

257   provinces, the two most economically developed regions in China. Hg abatement in these two

258   regions was mainly caused by the reduction of crude steel production, which was transferred

259   to nearby provinces such as Hebei, Zhejiang, Jiangsu, and Shandong. Thus, Hg emissions in

260   these nearby provinces all presented high AAGR of more than 10%. In 2015, the largest five

261   Hg emission provinces were changed to Hebei, Shandong, Henan, Jiangsu, and Shanxi

262   provinces. Emissions from these provinces reached 21.5 t, accounting for 68% of national

263   emissions. Liaoning, Jiangxi, Inner Mongolia, Gansu, and Shanghai were also in the list of the

264   top ten largest emitters.

265   3.2.3 Hg emission trends by species

266   Overall Hg speciation profile of ISP experienced great change during the study period,

267   from 50/44/6 (gaseous elemental Hg (Hg^0)/gaseous oxidized Hg (Hg^{II})/particulate-bound Hg

268   (Hg_p)) in 2000 to 40/59/1 in 2015 (**Fig. 4**). The proportion of Hg^{II} increased 15%, whereas

269   both Hg^0 and Hg_p proportion showed decreasing trend. Such shift indicated higher deposition

270   proportion of Hg around the emission points since Hg^{II} has larger deposition velocity and

271   higher water-solubility. For the long process steel making, Hg speciation profile shifted from

272   49/44/7 in 2000 to 39/60/1. The speciation shift in roasting plants was mainly impacted by the

273   replacement of WS and CYC with FF, which increased the emitted Hg^{II} proportion from 38%

274   to 75%. The replacement of indigenous coke production method with machine coke

275   production method mainly contributed to Hg^{II} proportion increase from 42% to 52% at first.

276   However, the gradual installation of WS in addition to cooler for air pollution control of

277   machine coke production method further washed Hg^{II} and reduced Hg^{II} proportion to 49% in

278   2015. Hg^{II} proportion in the exhaust gas of sinter/pellet plant has increased by 20%. The

279   increase of Hg^{II} proportion in sinter/pellet plant was mainly impacted by the substitute of WS

280   with ESP, FF, ESP+WFGD, or ESP+DFGD+FF which generally emitted gas with higher Hg^{II}

281   proportion (**Table S4**). Increase of Hg^{II} emission proportion in blast furnace was due to higher

282   Hg^{II} emission proportion after FF than venturi. In the oxygen steel making process, Hg

283   speciation profile almost unchanged. For the short process steel making, Hg^0 was the

284   dominant speciation during the whole study period and the proportion of Hg^0 increased from

285   66% in 2000 to 79% in 2015.

3.3 Uncertainty analysis

287   In 2015, overall uncertainty of atmospheric Hg emissions from ISP was in the range of

288   (-29%, 77%) (**Fig. 5**). Previous studies in ISP indicated the emission uncertainties of this

289   source were (-80%.100%) in the study of Zhang et al. (2015) and (-100%, 100%) in the study

290   of Streets et al. (2005) and Wu et al. (2006). The improvement of emission estimation of this

291   study was contributed by better knowledge on the Hg concentrations of raw materials and Hg

292   removal efficiencies of APCDs. In all ISP processes, the largest uncertainties existed in

293   emissions from roasting plant (-59%, 130%) and sinter/pellet process (-45%, 126%). These

294   mainly due to larger distribution range of Hg concentrations in limestone and iron ore as well

295   as Hg removal efficiencies of APCDs. The uncertainties of Hg emissions from other processes

296   were much lower, (-49%, 48%) for coke oven, (-23%, 46%) for blast furnace, (-41%, 27%)

297   for oxygen steel making, and (-60%, 54%) for arc steel making.

3.4 Comparison and implications

299   Due to the complicated ISP processes and limitations of data availability, the process

300   combinations considered in different inventories were divided into four types (**Fig. 6**)

301   (AMAP/UNEP, 2008, 2013; Wang K. et al., 2016; Wu et al., 2016; Wu et al., 2006; Zhang et

302   al., 2015a). The first type included sinter plant and blast furnace, which were the basic

303   assumption in the emission inventories of Wu et al. (2003), Zhang L. et al. (2015), and

304   AMAP/UNEP (2005). In these studies, unique emission factor of 0.0400 g/t was applied

305   (**Table S5**) and their emissions were similar in the same inventory year. Our emissions for this

306   process combination were almost the same as above estimations around 2005. However, the

307   gap grew with time when FGD was gradually applied in sinter/pellet plant. Therefore,

308   emission factor for this type of combination was reduced from 0.0527 g/t in 2000 to 0.0296

309   g/t in 2015 (**Table S5**). The second type also consisted of steel making in addition to the first

310   type. Our estimation was much higher than the study of Wang K. et al. (2016) because the

311   emission factors applied in Wang K.'s study were mainly derived from European technical

312   report (EMEP/CORINAIR, 2001; EMEP/EEA, 2013). However, the technology applied in

313   Europe may be better than China's situation. For example, the emission factor of 0.00019 g/t

314   applied for blast furnace with FF was used as best emission factor in Wang K.'s study (2016).

315   However, the combination of WS and venturi scrubber was the dominant APCD type for

316   China's blast furnace (Zhao et al., 2013), Hg removal efficiency of which was lower than that

317   of FF. The third type of process combination also included coke oven as part of ISP in

318   addition to the second type. Lower Hg emissions estimated by AMAP/UNEP (2013) were due

319   to their lower Hg concentration in coal. In addition, although different processes were

320   considered in the global report, unique APCD profile was applied for different process. The

321   application proportion of ESP+FGD reached 55%. However, FGD were mainly installed in

322   sinter/pellet plant but rarely applied in other processes. Thus, the emissions estimated by the

323   global report were lower than our estimation. The forth type also considered the emissions

324   from roasting process where emissions accounted for 9%-11% of total emissions.

325   The comparison of emissions from different types of process combination in this study

326   indicated the significance of including emissions from roasting plant and coke oven in the ISP

327   emission inventories. The proportion of emissions from these two processes accounted for

328   22%-34% of ISP's emissions during the whole study period. In addition, these two processes

329   were important in shaping the trends of ISP Hg emissions. For example, Hg emissions of all

330   processes showed an increase during 2007-2008 (Red line in Fig. 6). However, if these two

331   processes were not considered, we will observe a decreasing trend (Green and orange line in

332   Fig.6). Moreover, given the impact of APCDs on the emission estimation, inventories in ISP

333   should also apply distrinct APCD profiles for different processes so as to reduce the

334   uncertainty of inventories.

335   Future Hg emission for ISP was forecasted to decrease based on comprehensive

336   consideration of dominant parameters (e.g., steel production, air pollution control measures)

337   in the technology-based method and the emission trends from China's ISP during 2000-2015.

338   On one aspect, the annual growth rate of crude steel production reduced from 14.2% of

339   2000-2014 to 1.24% of 2015-2016. Thus, China's ISP has passed the quick growth period.

340   During 2014-2016, the crude steel production was around 810 Mt. It was expected the peak of

341   crude steel production was in the range of 669-1092 Mt (Zhong, 2013) and the crude steel

342   production in 2020 will ranged in 750-800 Mt (MIIT, 2016). Therefore, the peak of crude

343   steel production may have arrived or be coming. And slow decreasing crude steel production

344   was expected after the peak according to the development trends of mineral resources

345   consumption rule in developed countries. In addition, with the coming of high-yield-period of

346   steel scrap production (Guo and Wei, 2010), the application proportion of short process steel

347   making method is expected to increase, which will indirectly reduce the requirement of steel

348   production from long process steel making method. The replacement of steel production

349   method will also be one driver of Hg emission reduction considering lower Hg emission

350   factors of short process. Moreover, energy consumptions are required to be reduced by more

351   than 10% during the 2016-2020 (MIIT, 2016) and energy savings will be a long-term strategic

352   in China. The improvement of energy efficiency in the main processes will reduce energy

353   consumption (Li et al., 2015) and further lead to the reduction of Hg input. On the other

354   aspect, emissions of pollutants (eg., SO_2, NOx, and PM) are required to be reduced by at least

355   15% for ISP before 2020 in China (MIIT, 2016). To fulfill this goal, corresponding emission

356   standards have been issued (Wu, 2013), which will accelerate the applications of improved

357   APCDs. During 2010-2015, the increase of SO_2 emission limits from 1500 mg/m^3 to 200

358   mg/m^3 promoted the large-scale application of desulfurization devices in the sinter/pellet plant

359   of ISP. After 2015, ISP will move forward to NO_x control by using related technologies such

360   as selective catalytic reduction (SC, 2013), the synergic Hg removal efficiencies of which

361   have been proved in other industries (Wang et al., 2010). If we assumed that the crude steel

362   production reached a conservative value of 1000 Mt and that advanced dust collectors (ESP or

363 FF), desulfurization towers, and denitration technologies were fully applied in ISP,

364 atmospheric Hg emissions in ISP will be reduced to 27 t in 2020. Thus, a decreasing trend

365 will be expected from 2015 to 2020. Such conclusion is opposite with the study using

366 transformed normal distribution method (Wu et al., 2016). In this study, the transformed

367 normal distribution function was applied to estimate atmospheric Hg emissions from ISP. By

368 using such semi-quantitative method, the emission factor in 2020 (0.0402 g/t for long process

369 and 0.0211 g/t for short process) was almost the same as that in 2015 (0.0403 g/t for long

370 process and 0.0212 g/t for short process). Thus, atmospheric Hg emissions in 2020 will

371 almost depend on crude steel production and the emissions in 2020 will reach 40 t at the

372 conservative situation. Therefore, the technology-based emission factor method will provide

373 more objective forecast of future emissions.

374 **4 Conclusion**

375 In this study, atmospheric Hg emissions from ISP during 2000-2015 were estimated by

376 using technology-based emission factor method with up-to-date parameters. The input of Hg

377 as impurity of raw materials of ISP increased from 21.6 t in 2000 to 94.5 t in 2015. In the

378 various types of raw materials, coking coal and iron concentrates contributed to the largest

379 amount of Hg input, 35%-46% and 25%-31% of national total, respectively. Atmospheric Hg

380 emissions from ISP increased from 11.5 t in 2000 to the peak of 35.6 t in 2013, and then

381 reduced to 32.7 t in 2015. Overall Hg speciation shift from 50/44/6 (Hg^0/Hg^{II}/Hg_P) in 2000 to

382 40/59/1 in 2015. In the coming years, emissions from ISP are expected to decrease due to the

383 projection of Hg input reduction and improvement of APCDs.

384 In 2015, emissions from long process steel making method and short process steel

385 making were 32.2 t and 0.5 t, accounting for 98.3% and 1.7% of national total, respectively.

386 Sinter/pellet plant and blast furnace were the largest two emission processes, accounted for 49%

387 and 24% of national emissions, respectively. However, emissions from roasting and coke

388 oven should cause attention because their emissions accounted for 22% of national emissions.

389 The largest five Hg emission provinces were Hebei, Shandong, Henan, Jiangsu, and Shanxi

390 provinces. Emissions from these provinces reached 21.5 t, accounting for 68% of national

391 emissions.

392   In this study, we applied the technology-based emission factor method for better

393   quantification of Hg into ISP and atmospheric Hg emissions from different processes of ISP.

394   Compared with previous studies, the uncertainty of atmospheric Hg emissions from ISP has

395   largely reduced with better understanding of Hg flow in ISP. This method has provided more

396   objective estimation of current emissions and forecast of future emissions. However, with the

397   continuously change of APCD combinations, extensive and dedicated field experiments are

398   still required to generate suitable database of Hg removal efficiencies for the improved

399   APCDs in the future.

400   *Acknowledgment.* This study was supported by the Major State Basic Research Development
401   Program of China (973 Program) (2013CB430001), Natural Science Foundation of China
402   (21607090), and China Postdoctoral Science Foundation (2016T90103, 2016M601053)

403

404   **References**

405   Arctic Monitoring and Assessment Programme and United Nations Environment Programme
406   (AMAP/UNEP): Technical background report to the global atmospheric mercury
407   assessment, AMAP/UNEP, Geneva, Switzerland, 2008.
408   Arctic Monitoring and Assessment Programme and United Nations Environment Programme
409   (AMAP/UNEP): Technical background report for the global mercury assessment,
410   AMAP/UNEP, Geneva, Switzerland, 2013.
411   China Iron and Steel Industry Association (CISIA): China Steel yearbook, CISIA, Beijing,
412   China, 2001-2016.
413   European Monitoring and Evaluation Programme/Core Inventory of Air Emissions Project
414   (EMEP/CORINAIR): Emission inventory guidebook, EMEP/CORINAIR, Copenhagen,
415   Denmark, 2001.
416   European Monitoring and Evaluation Programme/European Economic Area (EMEP/EEA):
417   Air pollutant emission inventory guidebook 2013, EMEP/EEA, Copenhagen, Danmark,
418   2013.
419   Gao, W.: Study on atmospheric mercury emission characteristics for iron and steel producing
420   process in China, Tsinghua University, School of Environment, Beijing, China, 2016.
421   Guo, T., and Wei, L.: Development direction of the recycling industry of secondary zinc
422   resources, China Nonfer. Metal., 4, 2010.
423   Hui, M. L., Wu, Q. R., Wang, S. X., Liang, S., Zhang, L., Wang, F. Y., Lenzen, M., Wang, Y.
424   F., Xu, L. X., Lin, Z. T., Yang, H., Lin, Y., Larssen, T., Xu, M., and Hao, J. M.: Mercury
425   Flows in China and global drivers, Environ. Sci. Technol., 51, 222-231, 2016.
426   Li, X. C., Gao, X., and Jiang, X. D.: Analysis on potential of energy conservation of Chinese
427   steel industry in the 13th five-year period, The tenth annual conference of China steel
428   and the sixth annual academic conference of Baogang, Shanghai, Beijing, 2015-10-21,
429   2015.
430   Liu, H., Fu, M. L., Jin, X. X., Shang, Y., Shindell, D., Faluvegi, G., Shindell, C., and He, K.
431   B.: Health and climate impacts of ocean-going vessels in East Asia, Nature climate
432   change, 6, 1037-1041, 2016.
433   Ma, H. L.: China steel statistics, Development and Planning Division of Ministry of
434   Metallurgical, Beijing, China, 1995.
435   Ma, J.: Review and projection of technology development of lime used in China's steel
436   industry, China steel, 6, 17-20, 2011.
437   Ministry of Environmental Protection (MEP): "Twelfth Five-year" plan for the comprehensive
438   prevention and control of heavy metal pollution, MEP, Beijing, China, 2011.
439   Ministry of industry and information Technology (MIIT): Adjustment and upgrading plan of
440   iron and steel industry (2016-2020), MIIT, Beijing, China, 2016.
441   National Statistical Bureau of China (NBS): China Environmental Statistics Yearbook, NBS,
442   Beijing, China, 2001-2016.
443   National Energy Administration (NEA): Action plan of coal clean utilization, NEA, Beijing,
444   China, 2014.
445   National Energy Statistical Agency of China (NESA): China Energy Statistical Yearbook,
446   NESA, Beijing, China, 2001-2016.

State Council of the People's Republic of China (SC): Action plan of national air pollution prevention and control, SC, Beijing, China, 2013.

Streets, D. G., Hao, J. M., Wu, Y., Jiang, J. K., Chan, M., Tian, H. Z., and Feng, X. B.: Anthropogenic mercury emissions in China, Atmos. Environ., 39, 7789-7806, 2005.

Swaine, D. J.: Environmental aspects of trace-elements in coal, Environ. Geochem. Health, 14, 2-2, 1992.

Tao, S. R., and Wang, Y. J.: Imapct on the economic benefits of metallurgy industry from coke coal quality, Coal Proce. Compre. Utiliz., 4, 1994.

Tian, H. Z., Wang, Y., Xue, Z. G., Cheng, K., Qu, Y. P., Chai, F. H., and Hao, J. M.: Trend and characteristics of atmospheric emissions of Hg, As, and Se from coal combustion in China, 1980-2007, Atmos. Chem. Phys., 10, 11905-11919, 2010.

Tian, H. Z., Zhu, C. Y., Gao, J. J., Cheng, K., Hao, J. M., Wang, K., Hua, S. B., Wang, Y., and Zhou, J. R.: Quantitative assessment of atmospheric emissions of toxic heavy metals from anthropogenic sources in China: historical trend, spatial distribution, uncertainties, and control policies, Atmos. Chem. Phys., 15, 10127-10147, 2015.

United Nations Envieonment Programme (UNEP): Toolkit for identification and quantification of mercury releases. Guideline for inventory level 2, version 1.3. , 2013.

United States Environmental Portection Agency (US EPA): Method 7473: Hg in solids and solutions by thermal decomposition amalgamation and atomic absorption spectrophotometry, US EPA, Washinton D. C., United States, 1998.

United States Geological Survey (USGS): Mercury content in coal mines in China, Reston, Virginia, United States, 2004.

Wang, F. Y., Wang, S. X., Zhang, L., Yang, H., Gao, W., Wu, Q. R., and Hao, J. M.: Mercury mass flow in iron and steel production process and its implications for mercury emission control, J. Environ. Sci., 43, 293-301, 2016.

Wang, K., Tian, H. Z., Hua, S. B., Zhu, C. Y., Gao, J. J., Xue, Y. F., Hao, J. M., Wang, Y., and Zhou, J. R.: A comprehensive emission inventory of multiple air pollutants from iron and steel industry in China: Temporal trends and spatial variation characteristics, Sci. Total Environ., 559, 7-14, 2016.

Wang, S. X., Zhang, L., Li, G. H., Wu, Y., Hao, J. M., Pirrone, N., Sprovieri, F., and Ancora, M. P.: Mercury emission and speciation of coal-fired power plants in China, Atmos. Chem. Phys., 10, 1183-1192, 2010.

Wang, S. X., Zhao, B., Cai, S. Y., Klimont, Z., Nielsen, C. P., Morikawa, T., Woo, J. H., Kim, Y., Fu, X., Xu, J. Y., Hao, J. M., and He, K. B.: Emission trends and mitigation options for air pollutants in East Asia, Atmos. Chem. Phys., 14, 6571-6603, 2014.

Wang, Y. F.: Analysis on the harm of indigenous coking, Coal Eco. Res., 1, 1991.

Wu, Q. R., Wang, S. X., Zhang, L., Song, J. X., Yang, H., and Meng, Y.: Update of mercury emissions from China's primary zinc, lead and copper smelters, 2000-2010, Atmos. Chem. Phys., 12, 11153-11163, 2012.

Wu, Q. R., Wang, S. X., Li, G. L., Liang, S., Lin, C.-J., Wang, Y. F., Cai, S. Y., Liu, K. Y., and Hao, J. M.: Temporal trend and spatial distribution of speciated atmospheric mercury emissions in China during 1978–2014, Environ. Sci. Technol., 50, 13428-13435, 2016.

Wu, S. H.: Interpretation about "Emission Standards of Iron and Steel Industrial Pollutants", Indus. Safety Environ. Pro., 29, 2, 2013.

491   Wu, Y., Wang, S. X., Streets, D. G., Hao, J. M., Chan, M., and Jiang, J. K.: Trends in
492   anthropogenic mercury emissions in China from 1995 to 2003, Environ. Sci. Technol., 40,
493   5312-5318, 2006.

494   Zhang, L.: Emission characteristics and synergistic control strategies of atmospheric mercury
495   from coal combustion in China, Ph.D. Dissertation,Tsinghua University, School of
496   Environment, Beijing, China, 2012.

497   Zhang, L., Wang, S. X., Meng, Y., and Hao, J. M.: Influence of mercury and chlorine content
498   of coal on mercury emissions from coal-fired power plants in China, Environ. Sci.
499   Technol., 46, 6385-6392, 2012.

500   Zhang, L., Wang, S. X., Wang, L., Wu, Y., Duan, L., Wu, Q. R., Wang, F. Y., Yang, M., Yang,
501   H., Hao, J. M., and Liu, X.: Updated emission inventories for speciated atmospheric
502   mercury from anthropogenic sources in China, Environ. Sci. Technol., 49, 3185-3194,
503   2015a.

504   Zhang, Y. H., Zhang, C., Wang, D. Y., Luo, C., Yang, X., and Xu, F.: Characteristic of
505   mercury emissions and mass balance of the typical iron and steel industry, Environ. Sci.,
506   36, 8, 2015b.

507   Zhao, B., Wang, S. X., Liu, H., Xu, J. Y., Fu, K., Klimont, Z., Hao, J. M., He, K. B., Cofala, J.,
508   and Amann, M.: NOx emissions in China: historical trends and future perspectives,
509   Atmos. Chem. Phys., 13, 9869-9897, 2013.

510   Zhong, X. G.: Research on historical development and market forecast of China 's crude steel
511   production, Indus. Econo., 32-33, 2013.

512

 Tables

514 Table 1. Hg concentration in the raw materials

Province[1]	Iron ore				Limestone				Dolomite				Coking coal				PCI coal			
	AM[2]	MV[2]	SD[2]	NS[2]	AM	MV	SD	NS	AM	MV	SD	NS	AM	MV	SD	NS	AM	MV	SD	NS
	ng/g	ng/g	ng/g		ng/g	ng/g	ng/g		ng/g	ng/g	ng/g		ng/g	ng/g	ng/g		ng/g	ng/g	ng/g	
Tianjin	41	44	8	3	9	9		1	5	5	2	4					75	66	31	5
Hebei	37	24	40	79	374	117	631	27	7	8	5	5	78	66	39	71	79	85	70	38
Shanxi	30	24	28	25	9	7	8	6					77	71	27	22	114	106	19	3
Shanghai	44	44	50	4	20	20		1	39	39	2	2	125	152	71	5	12	12	0	2
Jiangsu					103	68	113	18												
Zhejiang					52	37	35	22												
Anhui	21	20	12	14	11	11	4	12	32	32	2	3	88	58	53	8	98	22	104	7
Fujian	19	14	11	15	11	11	5	4	9	8	5	4	105	100	51	13	255	239	51	7
Jiangxi	57	46	88	18					10	9	4	3	120	93	59	4	185	198	66	7
Shandong	125	128	73	20					24	24	1	2	72	69	21	12				
Henan	32	24	29	18	692	759	629	13												
Hubei					16	14	8	6					92	83	54	39	131	116	91	21
Hunan	33	19	34	77	102	87	62	4	3	3	1	2								
Guangdong					48	44	26	15												
Guangxi					8	8	2	4					210	188	112	27	96	98	30	6
Chongqing													85	79	48	20	65	65	12	4
Sichuan	37	2	44	7	10	9	4	12												
Guizhou					11	10	11	42												
Yunnan	10	10	7	6	17	20	7	6					51	52	7	8	58	56	6	3

Gansu	107	107	3	3	3	3		1					166	174	21	5	60	60	5	2
Xinjiang	6	5	4	17									82	82	46	22	31	24	19	15
National	38	20	48	306	153	18	402	204	14	9	12	25	99	82	68	256	99	73	83	120

515   Note: 1. Provinces without data were not listed in this table;

516   2. AM: Average mean; MV: Median value; SD: Standard deviation ; NS: Number of samples;

517   -.

518   Table 2. Provincial Hg emissions during 2000-2015

Province[1]	Atmospheric Hg emissions (kg)				
	2000	2005	2010	2015	AAGR
Beijing	432.0	316.1	132.9	0.0	-40%
Tianjin	260.0	482.0	863.4	688.9	7%
Hebei	1202.0	4016.0	6672.3	7129.3	13%
Shanxi	1587.3	2214.2	2075.2	1792.3	1%
Inner	287.5	477.8	667.7	753.8	7%
Liaoning	845.8	1171.1	1679.3	1563.4	4%
Jilin	109.5	190.9	282.8	267.9	6%
Heilongjiang	71.4	171.4	307.3	180.2	6%
Shanghai	1532.6	1155.7	1021.2	703.6	-5%
Jiangsu	304.5	1149.5	1891.4	2519.4	15%
Zhejiang	75.9	139.8	356.2	362.0	11%
Anhui	252.5	399.4	572.6	586.6	6%
Fujian	67.9	150.2	243.8	309.2	11%
Jiangxi	292.1	701.4	1054.0	984.8	8%
Shandong	1122.5	3965.4	6017.7	6051.1	12%
Henan	1259.8	2172.9	3495.3	4049.9	8%
Hubei	268.0	363.7	467.6	376.7	2%
Hunan	239.2	512.1	713.7	627.2	7%
Guangdong	131.7	286.6	339.7	395.9	8%
Guangxi	82.4	236.8	423.6	538.9	13%
Hainan	0.1	0.5	0.0	3.1	26%
Chongqing	106.2	121.7	168.4	142.3	2%
Sichuan	224.6	353.7	400.2	377.5	4%
Guizhou	100.9	235.4	204.1	187.4	4%
Yunnan	99.0	299.4	382.9	283.0	7%
Shaanxi	75.8	222.7	395.9	689.5	16%
Gansu	372.5	528.5	612.8	708.1	4%
Qinghai	12.2	10.6	64.5	24.8	5%
Ningxia	10.0	28.9	72.6	139.8	19%
Xinjiang	50.1	97.0	286.8	294.6	13%
Total	11476	22171	31866	32732	7%

519   Note: 1. Provinces without data were not listed in this table.

520 **Figures**
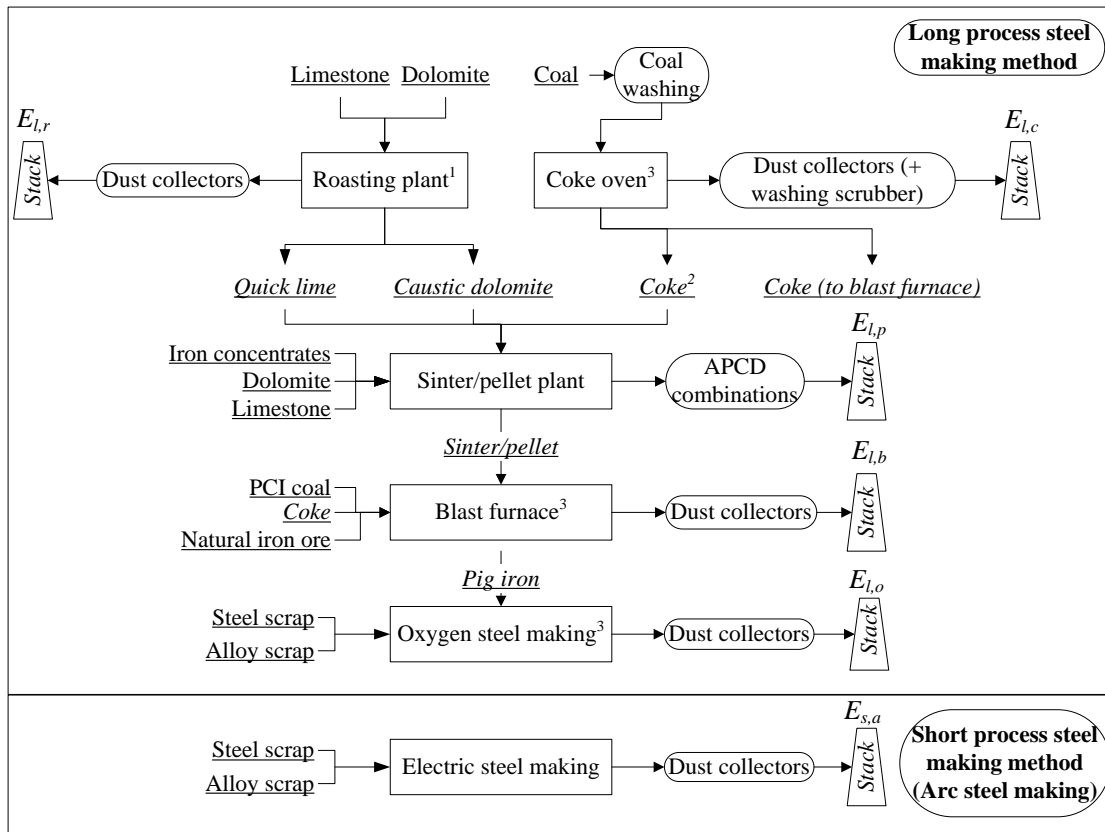
Note:1. Some plants roasted limestone and dolomite separately.
2. Mainly coke breeze. Some plants also use coal powder as fuel.
3. The flue gas after dust collectors are collected in gasometer before use.

521

522 **Fig. 1**. Flow chart of ISP processes
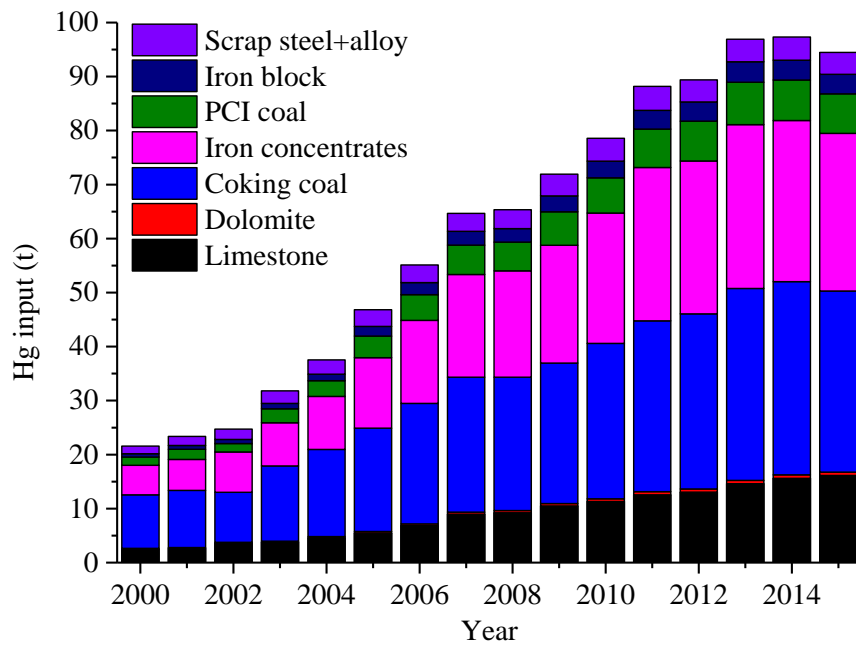
523

524 **Fig. 2**. Hg input trends by material
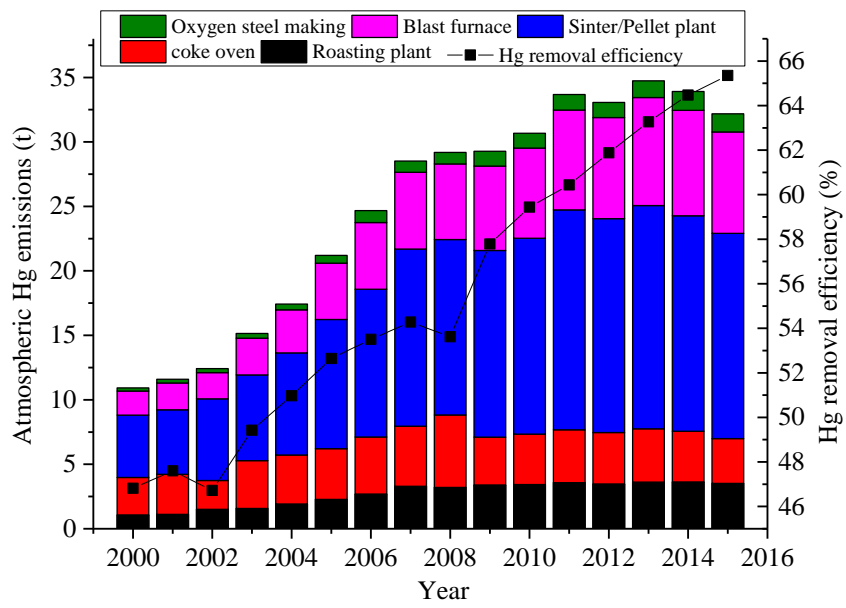
525

526   **Fig. 3**. Hg emission trends by process and Hg remvoal efficiency
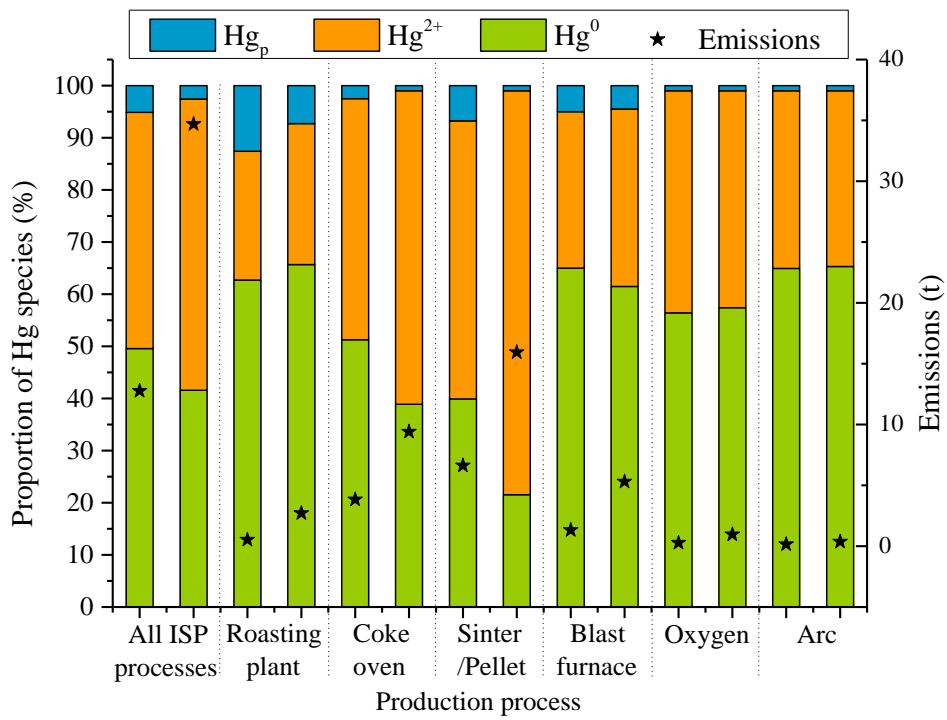
527

528 **Fig. 4**. Proportion of different Hg species (For each process, the left and right column

529 represents the data in 2000 and 2015, respectively)
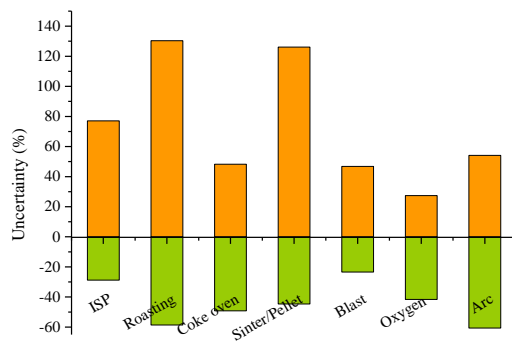
530

531   **Fig. 5**. Unertainty analysis

Red symbol: Sinter plant+blast furnace+roasting plant+coke oven+steel making
Blue symbol: Sinter plant+blast furnace+coke oven+steel making
Orange symbol: Sinter plant+blast furnace+steel making
Green symbol: Sinter plant+blast furnace
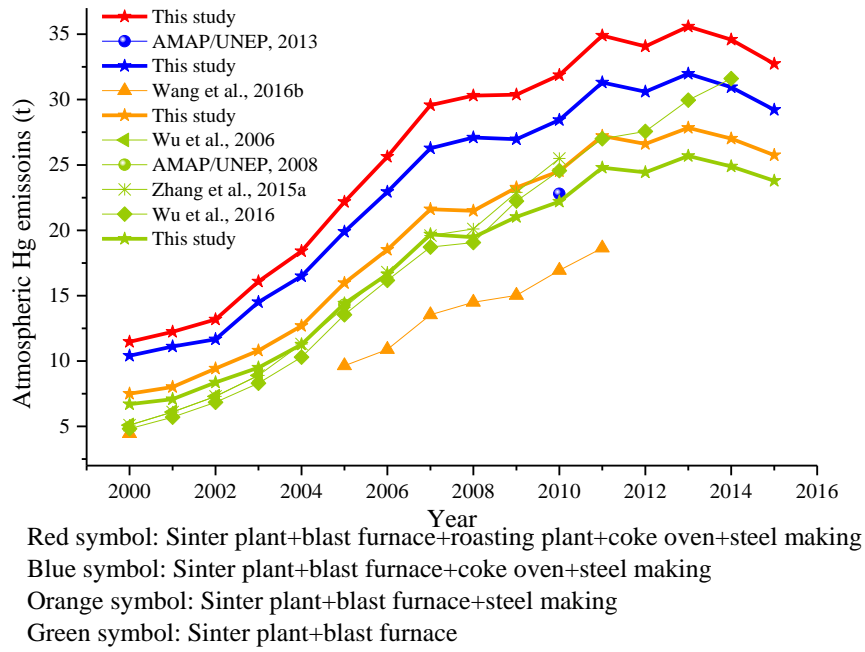
532

533   **Fig. 6**. Atmospheric Hg emissions of ISP in different studies

534